Supporting Information

Mg-IRMOF-74(*n*): A Novel Catalyst Series for
Hydrogen Activation and Hydrogenolysis of C-O Bonds

Vitalie Stavila,[†][*] Michael E. Foster,[†] Jonathan W. Brown,[†] Ryan W. Davis,[†] Jane Edgington,[†] Annabelle I. Benin,[†] Ryan A. Zarkesh,[†] Ramakrishnan Parthasarathi,[†] David W. Hoyt,[§] Eric D. Walter,[§] Amity Andersen,[§] Nancy M. Washton,[§] Andrew S. Lipton[§], Mark D. Allendorf[†][*]

[†]Chemistry, Combustion, and Materials Center, Sandia National Laboratories, Livermore, California 94551, United States

[§]Environmental Molecular Sciences Laboratory, Pacific Northwest National Laboratory, Richland, Washington 99354, United States

Table of Contents:

Table S1. Porosity-related properties of IRMOF-74(n)Mg catalysts.

	DFT pore diameter (nm)*	Pore volume (cm³/g)	N₂ BET Surface area (m²/g)	Density of OMS (nm⁻³)*
IRMOF-74(I)Mg	1.1	0.68	1627	4.52
IRMOF-74(II)Mg	1.7	0.91	1985	2.31
IRMOF-74(III)Mg	2.4	1.18	2413	1.53
IRMOF-74(IV)Mg	3.0	1.21	2448	1.00

*Computed from formula unit and cell volume reported by H. Deng et al., H. Deng, S. Grunder, K. E. Cordova, C. Valente, H. Furukawa, M. Hmadeh, F. Gándara, A. C. Whalley, Z. Liu, S. Asahina, H. Kazumori, M. O'Keeffe, O. Terasaki, J. F. Stoddart and O. M. Yaghi, Science, 2012, **336**, 1018-1023.*

Table S2. Ti and Ni metal content in IRMOF-74(n)Mg catalysts.

Catalyst	Ti or Ni metal loading (wt%)
TiCl$_x$@IRMOF-74(I)Mg	1.52
TiCl$_x$@IRMOF-74(II)Mg	1.75
TiCl$_x$@IRMOF-74(III)Mg	1.80
TiCl$_x$@IRMOF-74(IV)Mg	1.96
Ni@IRMOF-74(I)Mg	2.91
Ni@IRMOF-74(II)Mg	3.07
Ni@IRMOF-74(III)Mg	3.29
Ni@IRMOF-74(IV)Mg	3.43
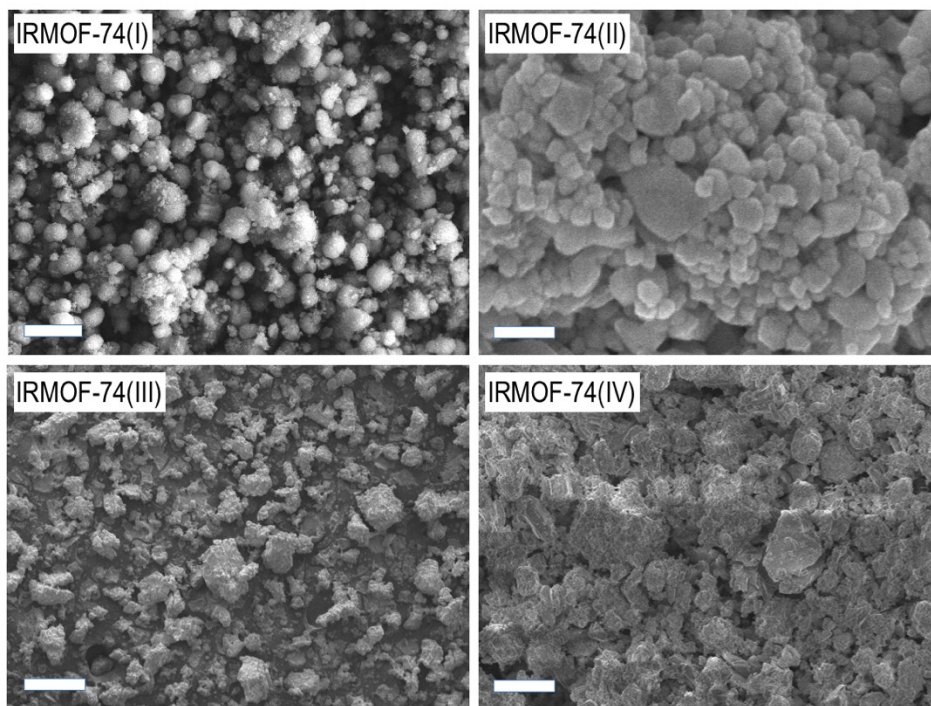
Figure S1A. SEM images for IRMOF-74(I-IV) catalysts showing micron and sub-micron particle sizes for all four catalysts. The scale bar in all cases is 2 microns.
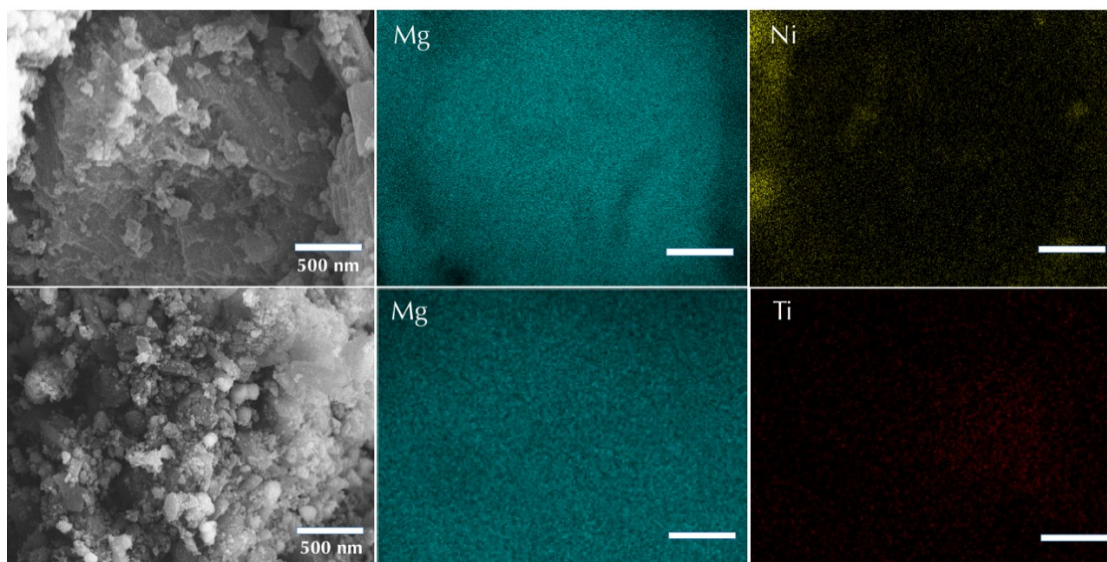
Figure S1B. SEM images and EDS maps for Ni- and Ti-doped IRMOF-74(III) showing homogeneous distribution of transition metals within the MOF matrix.
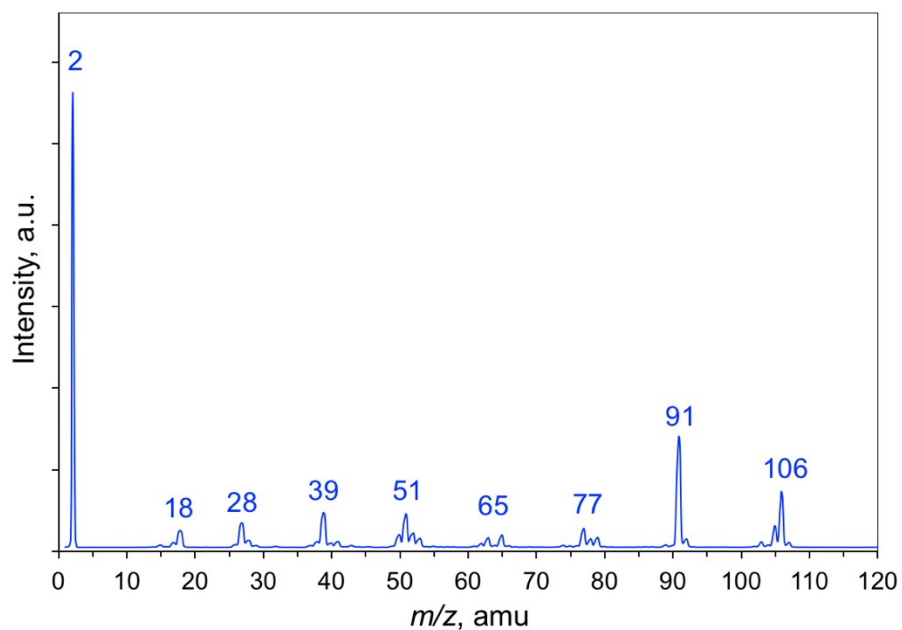
Figure S2. RGA spectrum of the reaction mixture resulting from the hydrogenolysis reaction of PPE in the presence of IRMOF-74(I). The peaks at m/z of 2, 18 and 28 are from H_2, H_2O, CO and/or N_2. The peaks at 39, 51, 65, 77, 91 and 106 are consistent with fragmentation patterns of ethylbenzene, phenol and *p*-xylene.
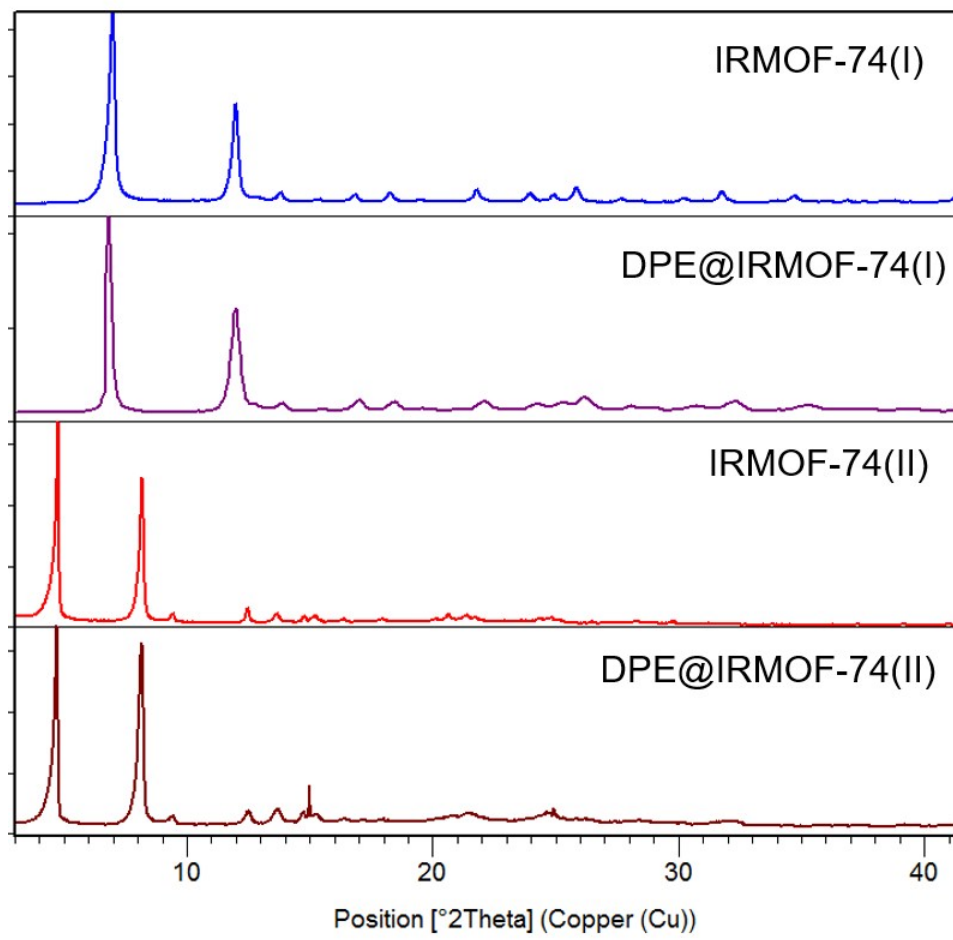
Figure S3. PXRD patterns of activated and DPE-loaded IRMOF-74(I) and IRMOF-74(II).
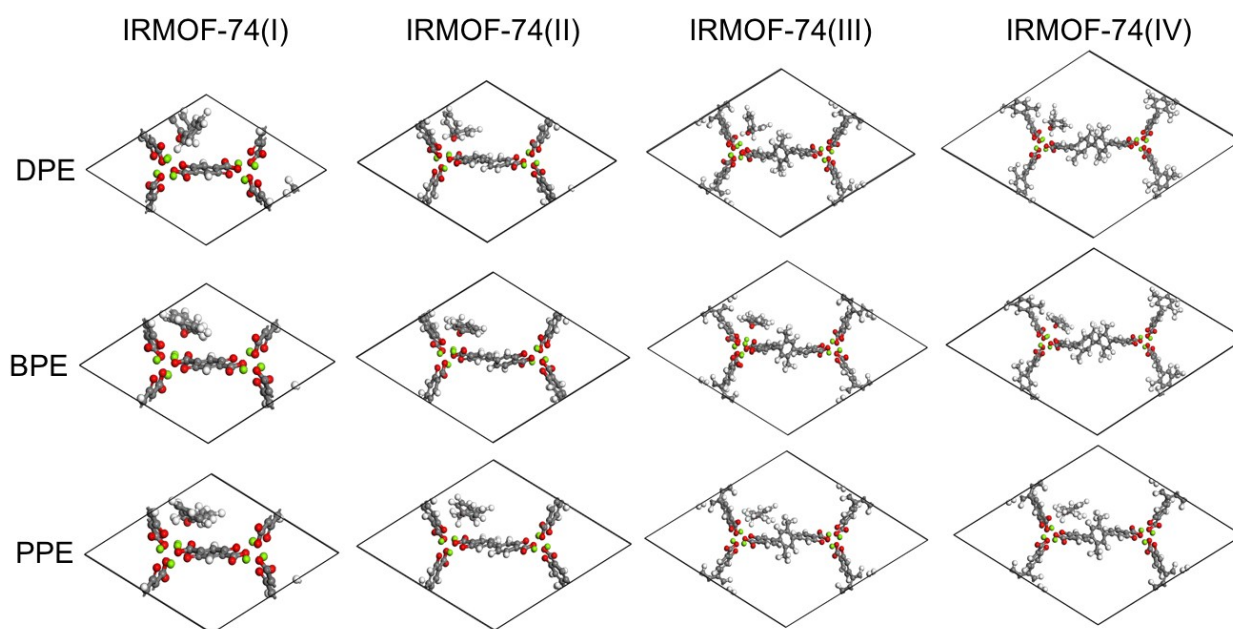
Figure S4. Optimized geometries showing the interactions of the PPE, BPE and DPE substrates with the IRMOF-74(I-IV) catalysts.

Solid State NMR Spectroscopy

Methodology. The local environments of Mg in IRMOF74 (I) was investigated by probing the metal with solid-state ^{25}Mg NMR. Due to the presence of multiple sites the quadrupole parameters extracted were verified by acquiring the data at two fields and fitting simultaneously. This allows the field dependence of the ^{25}Mg NMR lineshape to act as another constraint on the simulation. This helped determine that some of the signal extending on either side of the spectra collected at 20 T (850 MHz) resulted from signal of the outer transitions "leaking" into the desired central transition spectrum. There is precedent for this as observed in ^{67}Zn solid-state NMR (also a spin 5/2 nuclide with a similar gyromagnetic ratio).[1] The sample of IRMOF-74 with xylene and hydrogen gas was not available for NMR experiments at the second field so only a single field is presented. The quadrupole parameters extracted for this sample are therefore reported with less confidence than the others.

Simulations were performed using the SIMPSON (v3.1.0) simulation software package. Although the figures shown in this manuscript depict powder spectra the optimization was performed with calculations of the full QCPMG spectrum. The simulated powder spectra are presented here for clarity in visualization. The simulations were also performed with ideal pulses rather than finite pulses and stepped offset frequencies to increase the speed of the calculations. There was also no attempt to simulate any possible dynamics or exchange especially for the transient hydrogen gas or PPE substrate.

Analysis of spectra. The ^{25}Mg spectrum of the activated MOF is consistent with the previously reported results, in which two components were assigned as "ordered" and "disordered" magnesium centers.[52] The profile of the ordered centers is characterized by a broad peak with multiple shoulders, whereas the disordered peak is narrower and featureless. The observed spectra in Figure S10 are a composite of these. In the present work, we simulated the spectra corresponding to these using a C_q of 7.7 MHz and an asymmetry parameter (η) of 0.7 for 64% the "ordered" Mg(II) ions and a C_q of 2.8 MHz and η of 0.81 for the "disordered" center. We make this assignment based on the relative amounts in comparison with previously reported values for the activated MOF.[52] The previously reported ^{25}Mg spectra were simulated utilizing two similarly sized values of C_q, but when we performed the measurements at a second magnetic field strength (9.4 T), we found that the data do not support these values of C_q and η; i.e., simulating a 9.4 T spectrum utilizing the previously reported values does not describe the experimental data. The individual lineshapes for the spectra at both NMR field strengths are shown in the supporting information (Figure S5-S9).

Close examination of the ^{25}Mg spectra indicate that the addition of 1.5 MPa H2(g) and PPE produce changes to the spectrum indicative of new species (in the vicinity of the marker "B" in Figure S10). This new species also appears when a sample of MOF with *p*-xylene is pressurized with 15 bar hydrogen (again near the indicated "B"). The sample labeled "D-*p*-xylene + PPE" also shows the appearance of a second new species that we attribute to a PPE adduct having a C_q similar to the

species visible with only hydrogen gas and no xylene present. The spectrum of the (MOF + $H_{2(g)}$ + D-p-xylene + PPE) sample shows no obvious features corresponding to either the (MOF + $H_{2(g)}$) or (MOF + D-p-xylene + PPE) samples. We conclude that this spectrum is not simply a sum of the two spectra shown in Figure S10. These results suggest that when PPE and $H_{2(g)}$ are present simultaneously, the chemical environment around the Mg(II) OMS is altered in a manner different from when these reactants are present alone.

Table S3. Magnetic resonance parameters extracted from [25]Mg ssNMR.

Sample	Site	C_q (MHz)	η_q	δ_{iso} (ppm)	%
IRMOF-74(I)	1	7.68	0.70	-0.9	63.9
	2	2.82	0.81	5.7	36.1
IRMOF-74(I) + $H_{2(g)}$	1	7.76	0.70	02.4	47.3
	2	5.53	0.81	39.0	30.1
	3	2.65	0.93	-9.3	22.6
IRMOF-74(I) + $H_{2(g)}$ + xylene	1	8.19	0.50	15.5	51.9
	2	4.42	0.86	19.6	36.0
	3	2.46	0.96	-10.0	12.1
IRMOF-74(I) + PPE + xylene	1	7.41	0.70	-16.4	32.4
	2	5.61	0.97	16.6	46.7
	3	2.66	0.93	-1.7	20.9
IRMOF-74(I) + $H_{2(g)}$ + PPE + xylene	1	7.37	0.78	10.8	44.5
	2	5.47	0.96	17.6	36.7
	3	2.95	0.88	0.0	18.8
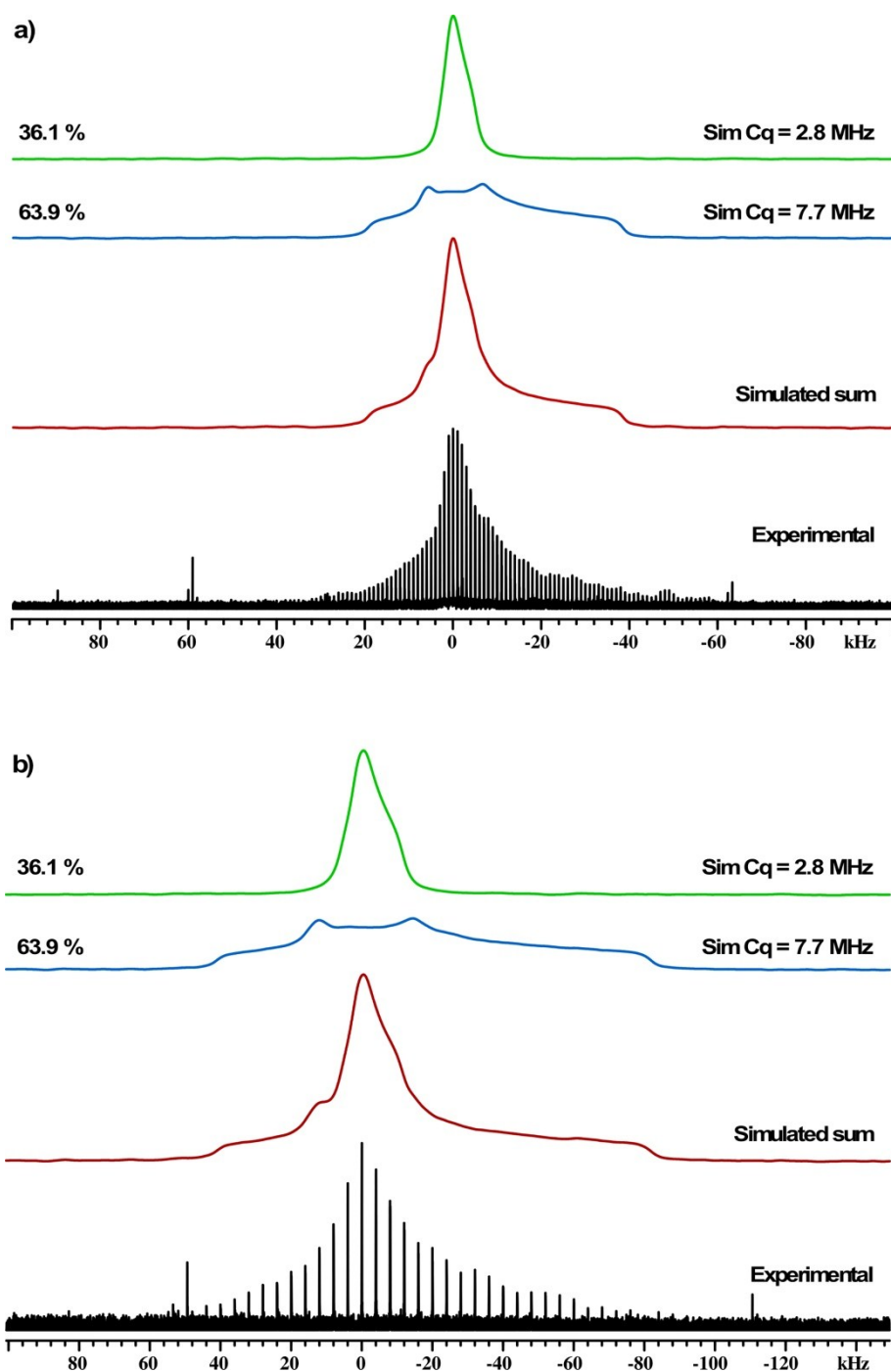
Figure S5. Experimental ^{25}Mg QCPMG spectrum (black) of activated IRMOF-74-I with simulated lineshapes of "ordered" (blue) and "disordered" (green) species with the sum (red) at (a) 20.05 T and (b) 9.4 T.

a)

22.6 %   Sim Cq = 2.7 MHz

30.1 %   Sim Cq = 5.5 MHz

47.3 %   Sim Cq = 7.8 MHz

                                          Simulated sum

                                          Experimental

| 80 | 60 | 40 | 20 | 0 | -20 | -40 | -60 | -80 | kHz |

b)

22.6 %   Sim Cq = 2.7 MHz

30.1 %   Sim Cq = 5.5 MHz

47.3 %   Sim Cq = 7.8 MHz

                                          Simulated sum

                                          Experimental

| 80 | 60 | 40 | 20 | 0 | -20 | -40 | -60 | -80 | -100 | -120 | kHz |
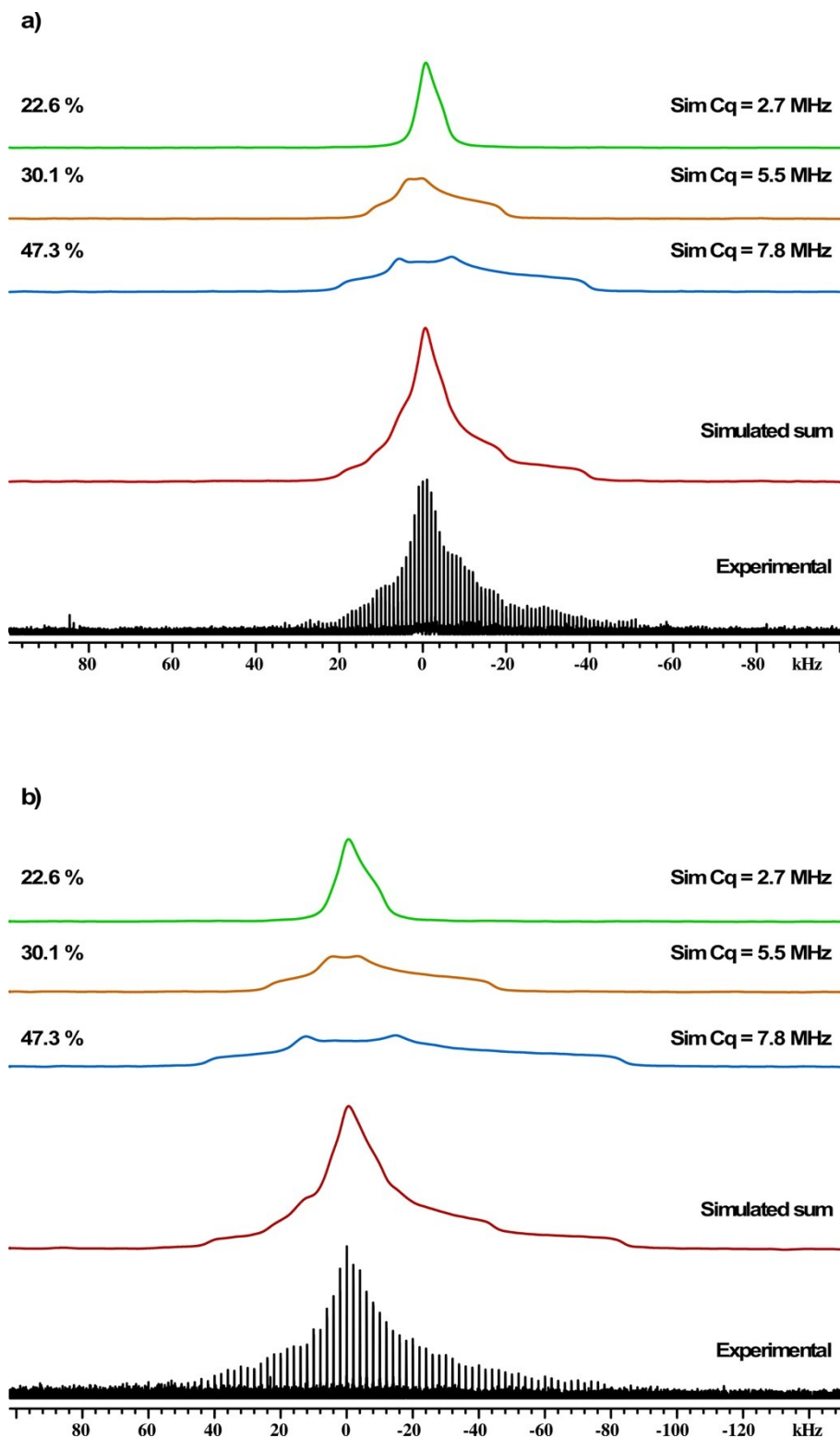
Figure S6. Experimental ^{25}Mg QCPMG spectrum (black) of activated IRMOF-74-I with 15 bar of hydrogen gas with simulated lineshapes of "ordered" (blue) and disordered (green) species with the sum (red) and a new species (orange)) at (a) 20.05 T and (b) 9.4 T.
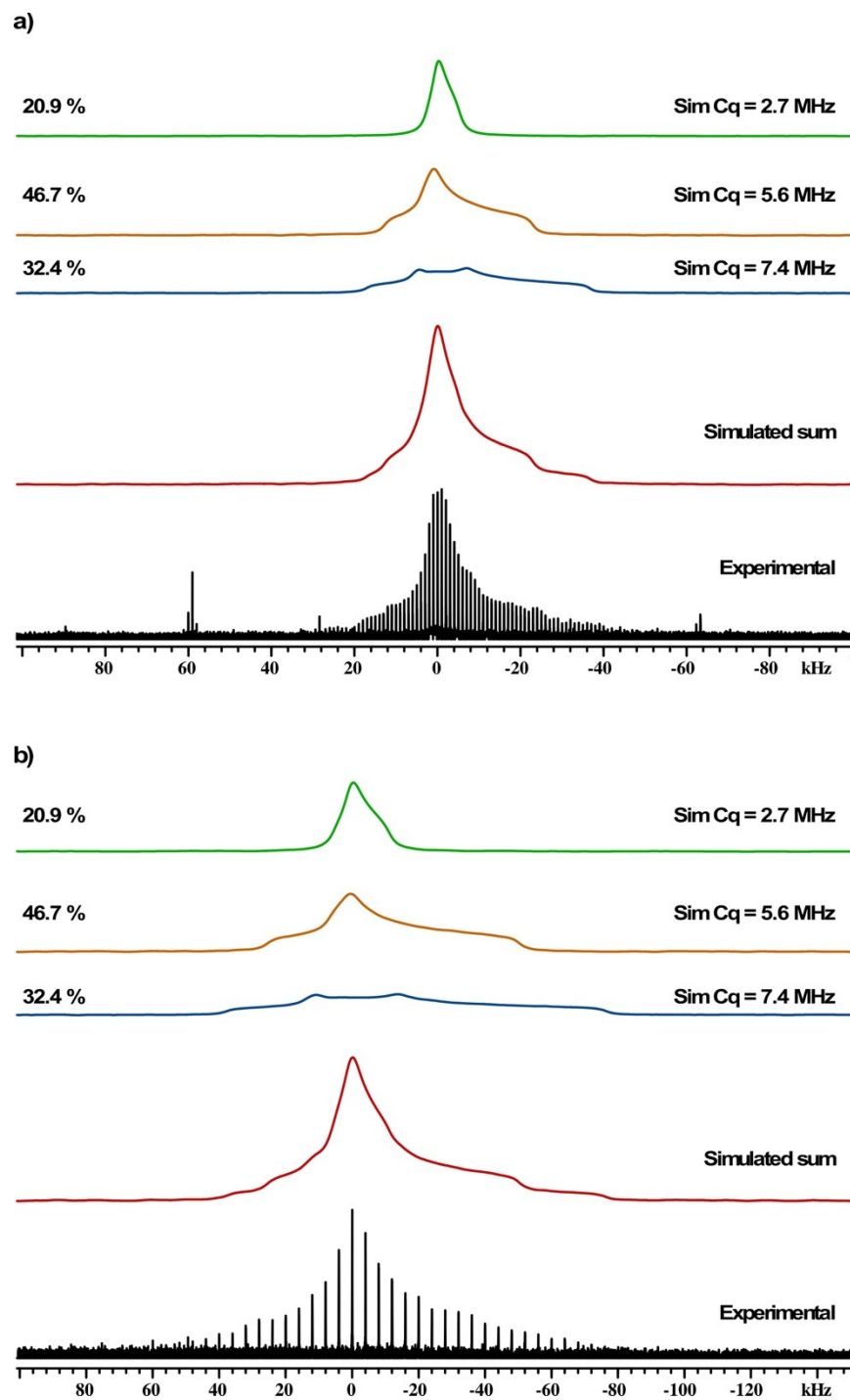
Figure S7. Experimental ^{25}Mg QCPMG spectrum (black) of activated IRMOF-74-I with deuterated *p*-xylene and PPE with simulated lineshapes of two new lineshapes (blue and purple) and the consistent "disordered" (green) species with the sum (red)) where the data was collected at (a) 20.05 T and (b) 9.4 T.
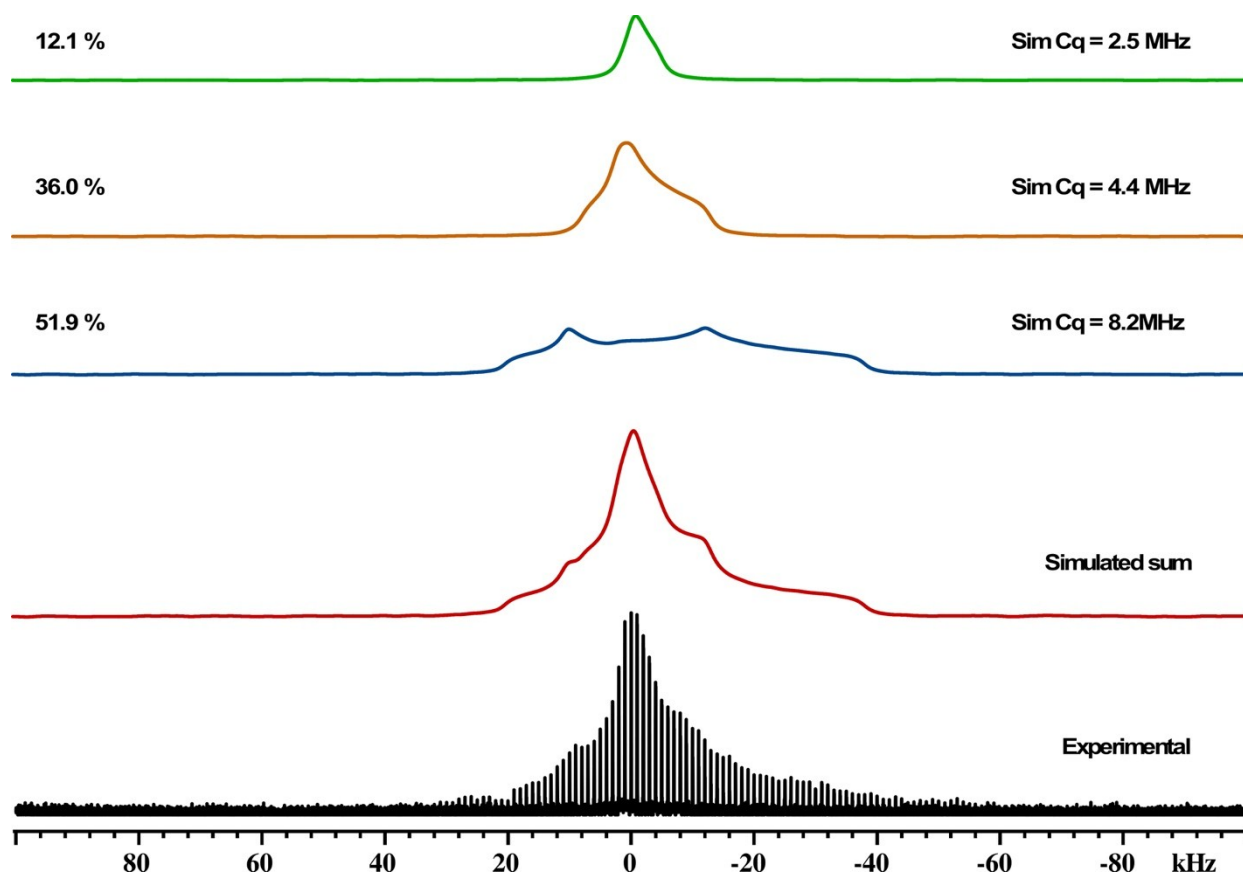
Figure S8. Experimental ^{25}Mg (20.05 T) QCPMG spectrum (black) of activated IRMOF-74-I with deuterated *p*-xylene and 15 bar $H_{2(g)}$ with simulated lineshapes of original "ordered" (blue), a species similar to what was observed in the absence of $H_{2(g)}$ (orange), a species similar to the MOF with only $H_{2(g)}$ (purple) and disordered (green) species with the sum (red).

a)

18.8 %　　　　　　　　　　　　　　　　　　　　Sim Cq = 3.0 MHz

36.7 %　　　　　　　　　　　　　　　　　　　　Sim Cq = 5.5 MHz

44.5 %　　　　　　　　　　　　　　　　　　　　Sim Cq = 7.4 MHz

　　　　　　　　　　　　　　　　　　　　　　　Simulated sum

　　　　　　　　　　　　　　　　　　　　　　　Experimental

```
     80      60      40      20       0      -20     -40     -60     -80    kHz
```

b)

18.8 %　　　　　　　　　　　　　　　　　　　　Sim Cq = 3.0 MHz

36.7 %　　　　　　　　　　　　　　　　　　　　Sim Cq = 5.5 MHz

44.5 %　　　　　　　　　　　　　　　　　　　　Sim Cq = 7.4 MHz

　　　　　　　　　　　　　　　　　　　　　　　Simulated sum

　　　　　　　　　　　　　　　　　　　　　　　Experimental

```
   80    60    40    20    0   -20   -40   -60   -80  -100  -120  kHz
```
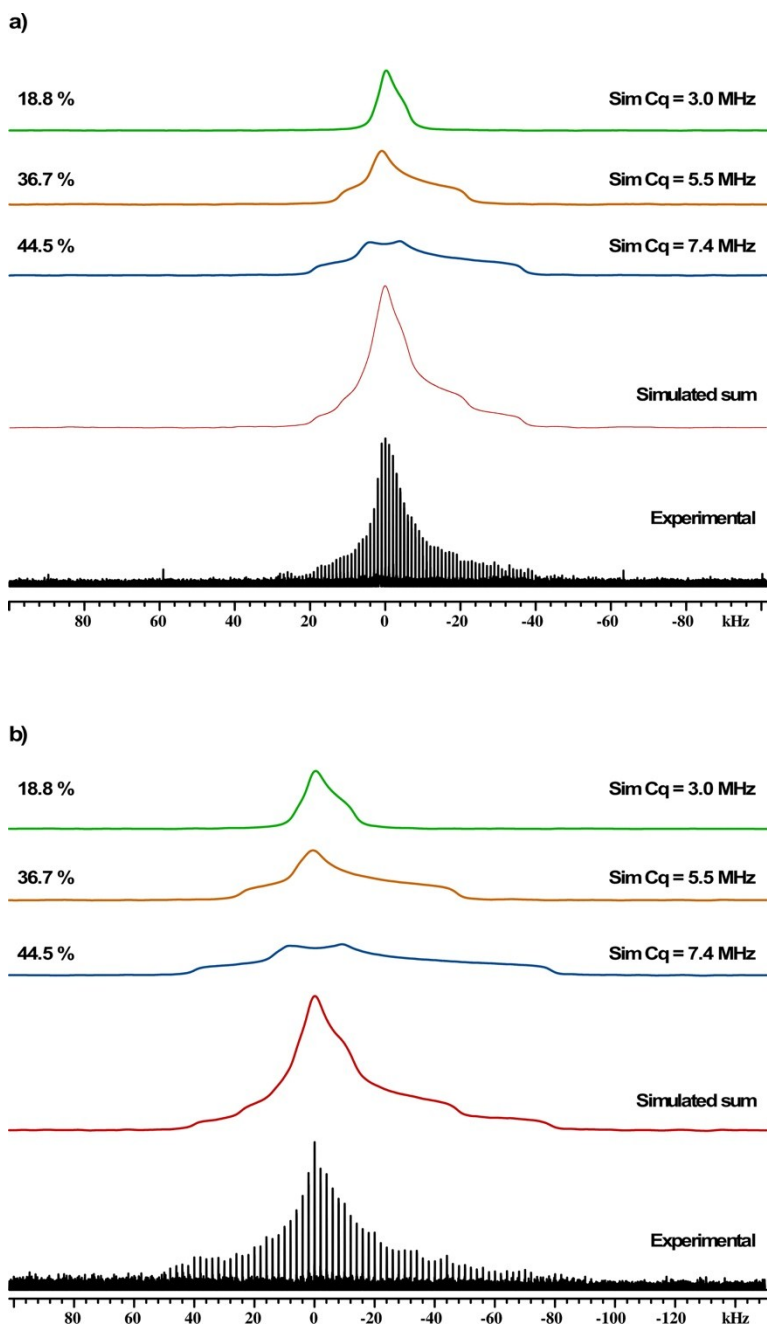
Figure S9. Experimental ^{25}Mg QCPMG spectrum (black) of activated IRMOF-74-I with deuterated *p*-xylene, PPE and 15 bar $H_{2(g)}$ with simulated lineshapes of original "ordered" (blue), a species similar to what was observed for solvated sample in the absence of $H_{2(g)}$ (orange), a species similar to the MOF with only $H_{2(g)}$ (purple) and disordered (green) species with the sum (red)) where the data was collected at (a) 20.05 T and (b) 9.4 T.
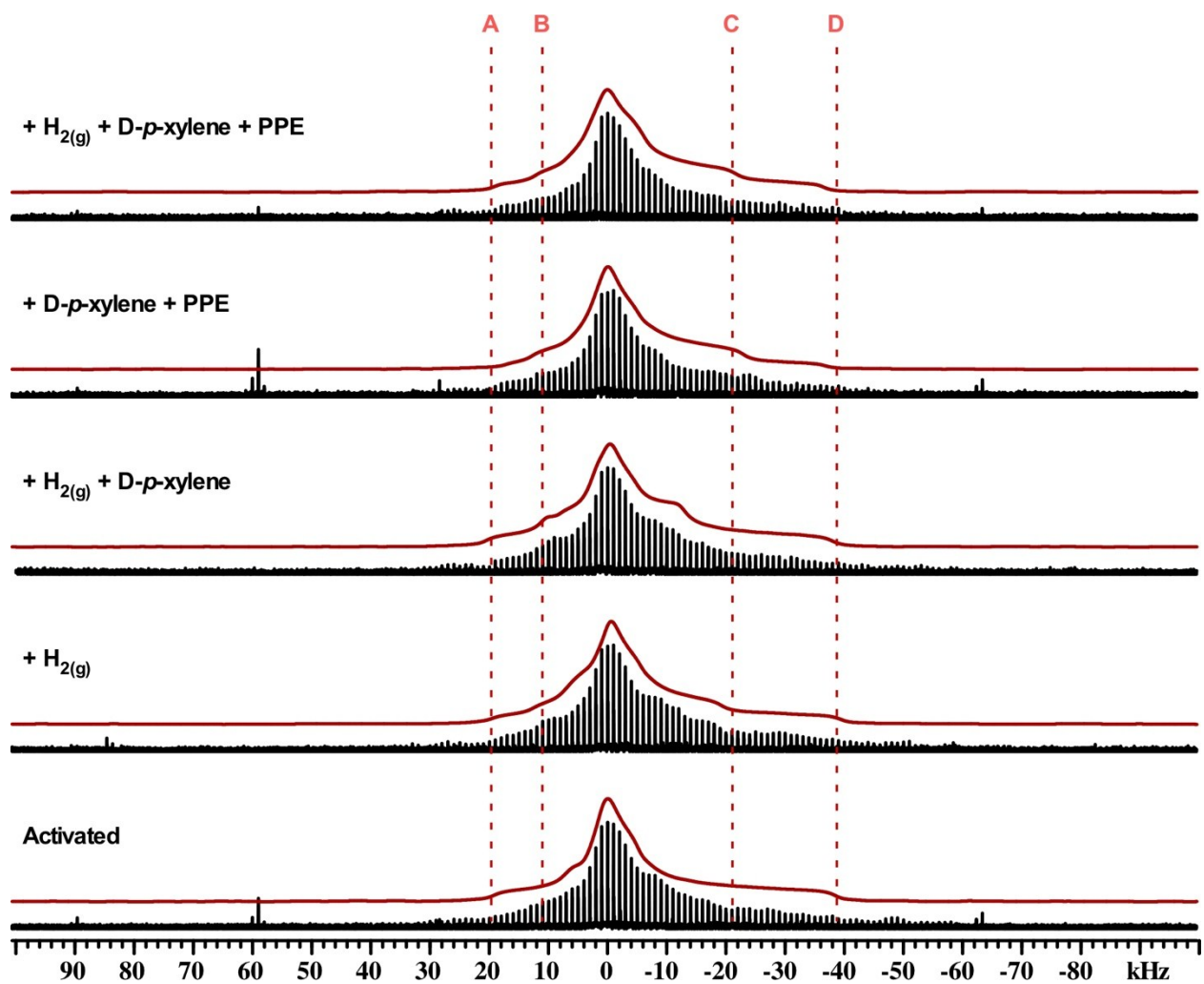
Figure S10. ^{25}Mg solid-state NMR spectra of the IRMOF-74(I)Mg catalyst (bottom) as a function of reaction step, in the presence of combinations of deuterated *p*-xylene, natural abundance PPE and under excess hydrogen gas as indicated. Features of note in the lineshapes are marked A, B, C and D.

Table S4. Effect of phenol on conversion efficiency of phenethyl phenyl ether (PPE) hydrogenolysis in the presence of IRMOF-74(I-IV) catalysts. The reactions were performed under 1 MPa H_2 pressure at 120 ºC for 16 hours. One equivalent of phenol was added at the beginning of the reaction.

Catalyst	Substrate	Conversion, %	Substrate	Conversion, %
IRMOF-74(I)	PPE	12	PPE + PhOH	13
IRMOF-74(II)	PPE	39	PPE + PhOH	32
IRMOF-74(III)	PPE	44	PPE + PhOH	35
IRMOF-74(IV)	PPE	35	PPE + PhOH	29

Reference:

1. A. S. Lipton, R. W. Heck, J. A. Sears and P. D. Ellis, *J Magn. Reson.*, 2004, **168**, 66-74.